



Contents lists available at ScienceDirect

Progress in Particle and Nuclear Physics

journal homepage: www.elsevier.com/locate/ppnp

Review

Indirect detection of dark matter, current status and recent results

A. Morselli

INFN, Roma Tor Vergata, Italy

ARTICLE INFO

Keywords:

Dark matter
Gamma-rays
Astroparticle

ABSTRACT

Since its launch in 2008, the Large Area Telescope, onboard the Fermi Gamma-ray Space Telescope, has detected the largest amount of gamma rays, in the 20 MeV–300 GeV energy range and electrons + positrons in the 7 GeV–1 TeV range. These impressive statistics allow one to perform a very sensitive indirect experimental search for dark matter. I will present the latest results on these searches.

© 2011 Elsevier B.V. All rights reserved.

1. The cosmic ray electron spectrum

Recently the experimental information available on the Cosmic Ray Electron (CRE) spectrum has been dramatically expanded as the Fermi-LAT Collaboration [1,2] has reported a high precision measurement of the electron spectrum from 7 GeV to 1 TeV performed with its Large Area Telescope (LAT) [3,4]. The spectrum shows no prominent spectral features and it is significantly harder than that inferred from several previous experiments. These data together with the PAMELA data on the rise above 10 GeV of the positron fraction [5] are quite difficult to explain with just secondary production [6–8]. The temptation to claim the discovery of dark matter is strong but there are competing astrophysical sources, such as pulsars, that can give a strong flux of primary positrons and electrons (see [9–12] and references therein). At energies between 100 GeV and 1 TeV the electron flux reaching the Earth may be the sum of an almost homogeneous and isotropic component produced by Galactic supernova remnants and the local contribution of a few pulsars with the latter expected to contribute more and more significantly as the energy increases.

Two pulsars, Monogem, at a distance of $d = 290$ pc and Geminga, at a distance of $d = 160$ pc, can give a significant contribution to the high energy electron and positron flux reaching the Earth and with a set of reasonable parameters of the model of electron production we can have a nice fit of the PAMELA positron fraction [5] and Fermi data (see Figs. 1 and 2). However we have a lot of freedom in the choice of these parameters because we still do not know much about these processes, so further study on high energy emission from pulsars is needed in order to confirm or reject the pulsar hypothesis.

Nevertheless a dark matter interpretation of the Fermi-LAT and of the PAMELA data is still an open possibility. In Fig. 3 is shown the parameter space of dark matter particle mass versus pair-annihilation rate, for models where dark matter annihilates into monochromatic e^\pm [12]. The preferred range for the dark matter mass lies between 400 GeV and 1–2 TeV, with larger masses increasingly constrained by the H.E.S.S. results. The required annihilation rates, when employing a particular dark matter density profile imply typical boost factors ranging between 20 and 100, when compared to the value $\langle\sigma v\rangle \sim 3 \times 10^{-26}$ cm³/s expected for a thermally produced dark matter particle relic.

How can one distinguish between the contributions of pulsars and dark matter annihilations? Most likely, a confirmation of the dark matter signal will require a consistency between different experiments and new measurements of the reported excesses with large statistics. The observed excess in the positron fraction should be consistent with corresponding signals in absolute positron and electron fluxes in the PAMELA data and all lepton data collected by Fermi. Fermi has a large effective area and long projected lifetime, 5 years nominal with a goal 10 years mission, which makes it an excellent detector of

E-mail address: aldo.morselli@roma2.infn.it.

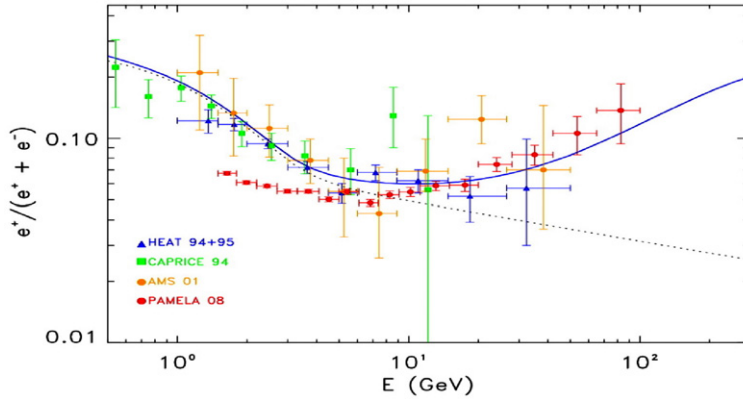


Fig. 1. PAMELA data and a possible contribution from Monogem and Geminga pulsars [12]. Black-dotted line shows the background from secondary positrons in cosmic rays from GALPROP.

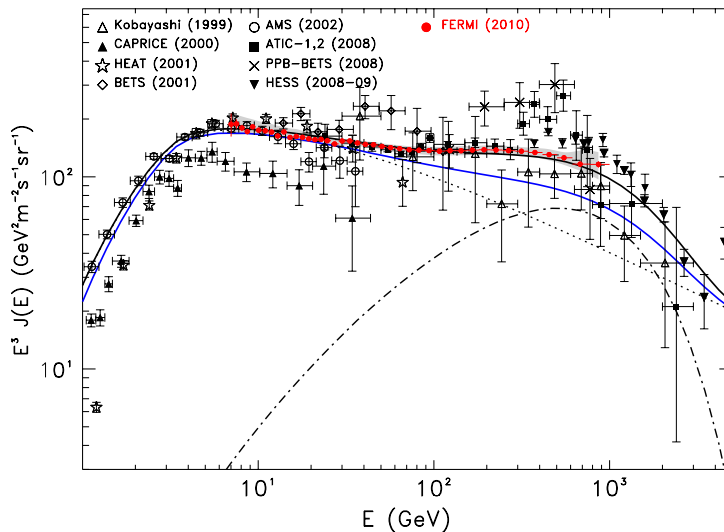


Fig. 2. Electron-plus-positron spectrum (blue continuous line) for the same scenario as in Fig. 1. The gray band represents systematic errors on the Fermi-LAT data [3,4].

cosmic-ray electrons up to ~ 1 TeV. Future Fermi measurements of the total lepton flux with large statistics make possible to distinguish a gradual change in slope with a sharp cutoff with high confidence [13]. The latter, can be an indication in favor of the dark matter hypothesis.

Another possibility is to look for anisotropies in the arrival direction of the electrons.

The Large Area Telescope on-board the *Fermi* satellite (*Fermi*-LAT) detected more than 1.6 million cosmic-ray electrons/positrons with energies above 60 GeV during its first year of operation. The arrival directions of these events were searched for anisotropies of angular scale extending from $\sim 10^\circ$ up to 90° , and of minimum energy extending from 60 up to 480 GeV. The upper limit for the dipole anisotropy has been set to 0.5%–5% depending on the energy [14].

The levels of anisotropy expected for Vela-like and Monogem-like sources (i.e. sources with similar distances and ages) seem to be higher than the scale of anisotropies excluded by the results (see Fig. 4). However, it is worth to point out that the model results are affected by large uncertainties related to the choice of the free parameters.

2. The gamma-ray signals

A strong leptonic signal should be accompanied by a boost in the γ -ray yield providing a distinct spectral signature detectable by Fermi.

The Galactic Center (GC) is expected to be the strongest source of γ -rays from DM annihilation, due to its coincidence with the cusped part of the DM halo density profile [15,16]. A preliminary analysis of the data, taken during the first 11 months of the Fermi satellite operations, is shown in Figs. 5 and 6.

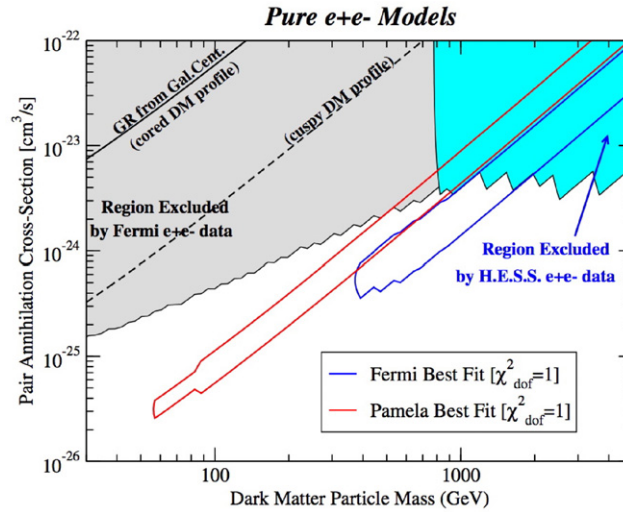


Fig. 3. The parameter space of dark matter particle mass versus pair-annihilation rate, for models where dark matter annihilates into monochromatic e^\pm . Models inside the regions shaded in gray and cyan over-produce e^\pm from dark matter annihilation with respect to the Fermi-LAT and H.E.S.S. measurements, at $2\text{-}\sigma$ level. The red and blue contours outline the regions where the χ^2 per degree of freedom for fits to the PAMELA and Fermi-LAT data is at or below 1.

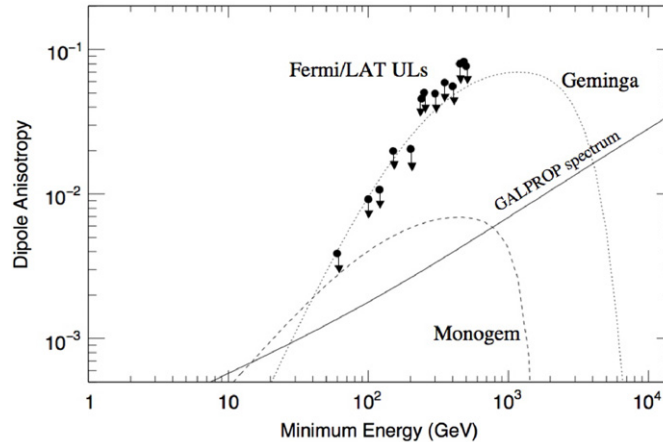


Fig. 4. Dipole anisotropy δ versus the minimum energy for GALPROP (solid line), Monogem source (dashed line), and Vela source (dotted line). The 3σ confidence level from the data is also shown with circles. The solar modulation was treated using the force-field approximation with $\Phi = 550$ MV.

The reported results were obtained with a binned likelihood analysis, performed by means of the tools developed by the Fermi/LAT collaboration (gtlike, from the Fermi analysis tools [17]). For this analysis:

- a ROI of $7^\circ \times 7^\circ$ was considered. This ROI was used in order to minimize the background contribution and to avoid significant leakage of the gamma ray signal under study;
- the ROI was centered at the position $RA = 266.46^\circ$, $Dec = -28.97^\circ$, i.e. the position of the brightest source;
- the data taken during the first 11 months (8/2008–7/2009) have been used;
- the events were selected to have an energy between 400 MeV and 100 GeV;
- only events classified as “diffuse” class and which converted in the *front* part of the tracker have been selected for the analysis. The selection in energy, event classification and conversion provided us with events with very well reconstructed incoming direction and data have been binned into a 100×100 bins map;
- the IRF and the events classification are those relative to the Pass6V3 version of the Fermi/LAT analysis software.

In order to perform the likelihood analysis for the LAT data, a model of the already known sources and the diffuse background should be built. The model in use for the presented analysis contains 11 sources in the Fermi 1 year catalog [18] which are located into or very close to the considered ROI. These sources have a point-like spatial model and a spectrum in the form of a power-law. The model also contains the diffuse gamma-ray background which is made of two components:

1. the Galactic Diffuse gamma-ray background. The observed Galactic Diffuse emission was modeled by means of the GALPROP code [19,20], and the realization of the Galactic emission named gll_iem_54_87Xexph7S.fit was used. During the likelihood maximization only the normalization of the GALPROP model is varied, not its components;

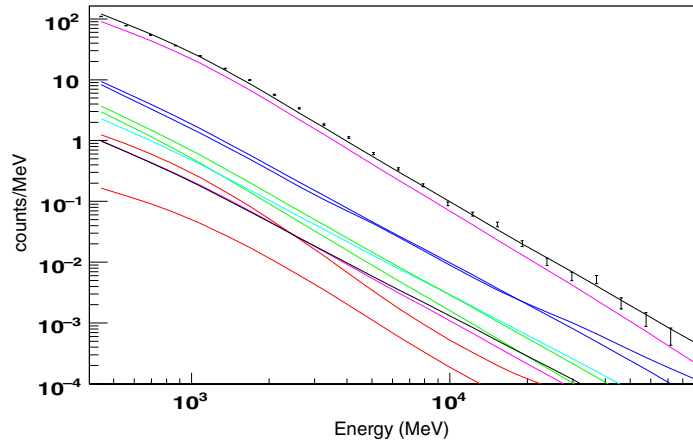


Fig. 5. Spectra from the likelihood analysis of the Fermi/LAT data (number of counts vs reconstructed energy) in a $7^\circ \times 7^\circ$ region around the Galactic Center (number of counts vs reconstructed energy). The likelihood analysis is the standard one used with the LAT data. The main analysis steps are: (1) to select data of high quality (selection cuts on events energy, zenith angle, reconstruction and classification quality); (2) to build an emission model of the region, based on the previous knowledge and experimental evidence of new excesses with enough statistical significance; (3) to apply the likelihood analysis to the data and the considered model. For each model component a fit of the free parameters and the computation of the statistical significance is obtained. Here in the plot, from above to below: the black points are the observed data; the black line is the sum of all the components; the red line is the Galactic Diffuse emission; the lower black line is the isotropic extragalactic; other components are the sources detected. These results are preliminary.

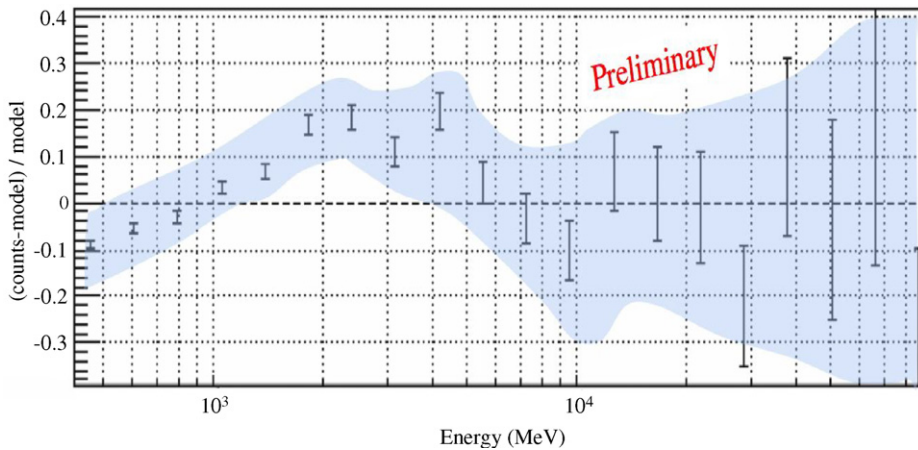


Fig. 6. Residuals $((\text{exp.data} - \text{model})/\text{model})$ of the above likelihood analysis. The blue area shows the systematic errors on the effective area. These results are preliminary.

2. the Isotropic Background. This component should account for both the Extragalactic gamma-ray emission and residual charged particles. It is modeled as an isotropic emission with a template spectrum.

The diffuse gamma-ray backgrounds and discrete sources, as we know them today, can account for the large majority of the detected gamma-ray emission from the Galactic Center. Nevertheless a residual emission is left, not accounted for by the above models [21].

Improved modeling of the Galactic Diffuse model as well as the potential contribution from other astrophysical sources (for instance unresolved point sources) could provide a better description of the data. Analyses are under-way to investigate these possibilities.

An excess in gamma-ray should also be seen in the Galactic diffuse spectrum.

In Fig. 7 it is shown the diffuse γ -rays in a mid-latitude region in the third quadrant (Galactic longitude l from 200° to 260° and latitude $|b|$ from 22° to 60°). The region contains no known large molecular clouds and most of the atomic hydrogen is within 1 kpc of the solar system. The contributions of γ -ray point sources and inverse Compton scattering are estimated and subtracted. The residual γ -ray intensity exhibits a linear correlation with the atomic gas column density in energy from 100 MeV to 10 GeV. The differential emissivity from 100 MeV to 10 GeV agrees with calculations based on cosmic ray spectra consistent with those directly measured, at the 10% level. The results obtained indicate that cosmic ray nuclei spectra within 1 kpc from the solar system in regions studied are close to the local interstellar spectra inferred from direct measurements at the Earth within $\sim 10\%$ [22].

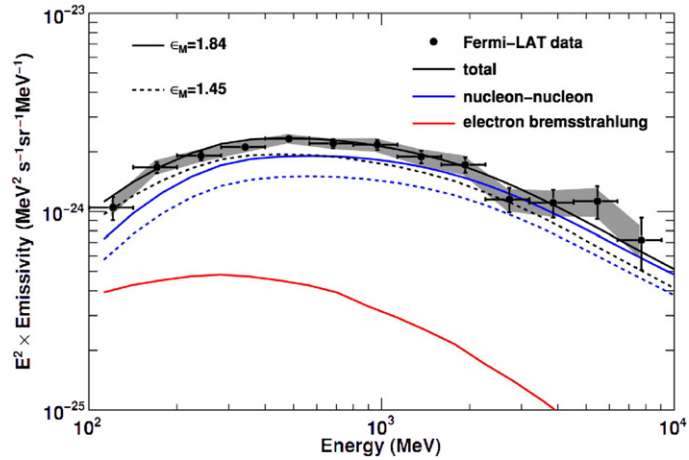


Fig. 7. Differential γ -ray emissivity from the local atomic hydrogen gas compared with the calculated γ -ray production. The horizontal and vertical error bars indicate the energy ranges and 1σ statistical errors, respectively. Estimated systematic errors of the LAT data are indicated by the shaded area. A nucleus enhancement factor ϵ_M of 1.84 is assumed for the calculation of the γ -rays from nucleon–nucleon interactions. Dotted lines indicate the emissivities for the case of $\epsilon_M = 1.45$, the lowest values in the referenced literature.

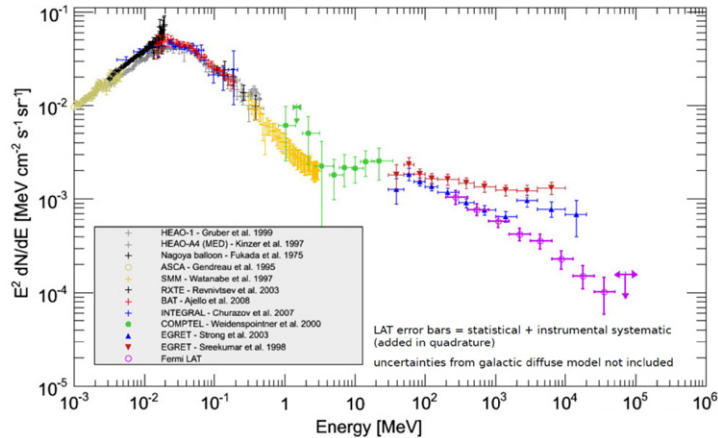


Fig. 8. Fermi-LAT extragalactic intensity compared with EGRET-derived intensities. Fermi-LAT derived spectrum is compatible with a simple power-law with index $\gamma = 2.41 \pm 0.05$ and intensity $I(>100 \text{ MeV}) = (1.03 \pm 0.17) \times 10^{-5} \text{ cm}^{-2} \text{ s}^{-1} \text{ sr}^{-1}$ where the uncertainties are systematics dominated.

The high-energy diffuse γ -ray emission is dominated by γ -rays produced by cosmic rays (CR) interacting with the Galactic interstellar gas and radiation fields, the so-called diffuse Galactic emission. A much fainter component, commonly designated as “extragalactic γ -ray background” (EGB) by definition has an isotropic sky distribution and is considered by many to be the superposition of contributions from unresolved extragalactic sources including active Galactic nuclei, starburst galaxies and γ -raybursts and truly-diffuse emission processes.

Fig. 8 shows the spectrum of the EGB above 200 MeV derived with the data taken during the first 11 months [23], and from EGRET data [24,25]. Our intensity extrapolated to 100 MeV based on the power-law fit, $I(>100 \text{ MeV}) = (1.03 \pm 0.17) \times 10^{-5} \text{ cm}^{-2} \text{ s}^{-1} \text{ sr}^{-1}$, is significantly lower than that obtained from EGRET data: $I_{\text{EGRET}}(>100 \text{ MeV}) = (1.45 \pm 0.05) \times 10^{-5} \text{ cm}^{-2} \text{ s}^{-1} \text{ sr}^{-1}$. Furthermore, our spectrum is compatible with a featureless power law with index $\gamma = 2.41 \pm 0.05$. This is significantly softer than the EGRET spectrum with index $\gamma_{\text{EGRET}} = 2.13 \pm 0.03$. To check that the different spectra are not due to the instrumental point-source sensitivities, we adopt $F(>100 \text{ MeV}) = 10^{-7} \text{ cm}^{-2} \text{ s}^{-1}$, comparable to the average EGRET sensitivity, and attribute the flux of all detected LAT sources below this threshold to the EGB. We obtain an intensity $I_{\text{res}}(>100 \text{ MeV}) = (1.19 \pm 0.18) \times 10^{-5} \text{ cm}^{-2} \text{ s}^{-1} \text{ sr}^{-1}$ and a spectrum compatible with a power-law with index $\gamma_{\text{res}} = 2.37 \pm 0.05$. Therefore, the discrepancy cannot be attributed to a lower threshold for resolving point sources. Our EGB intensity is comparable to that obtained in the EGRET re-analysis by [25] with an updated DGE model, $I_{\text{SMR}}(>100 \text{ MeV}) = (1.11 \pm 0.1) \times 10^{-5} \text{ cm}^{-2} \text{ s}^{-1} \text{ sr}^{-1}$. However, our EGB spectrum does not show the distinctive harder spectrum above $\geq 1 \text{ GeV}$ and peak at $\sim 3 \text{ GeV}$ found in the same EGRET re-analysis.

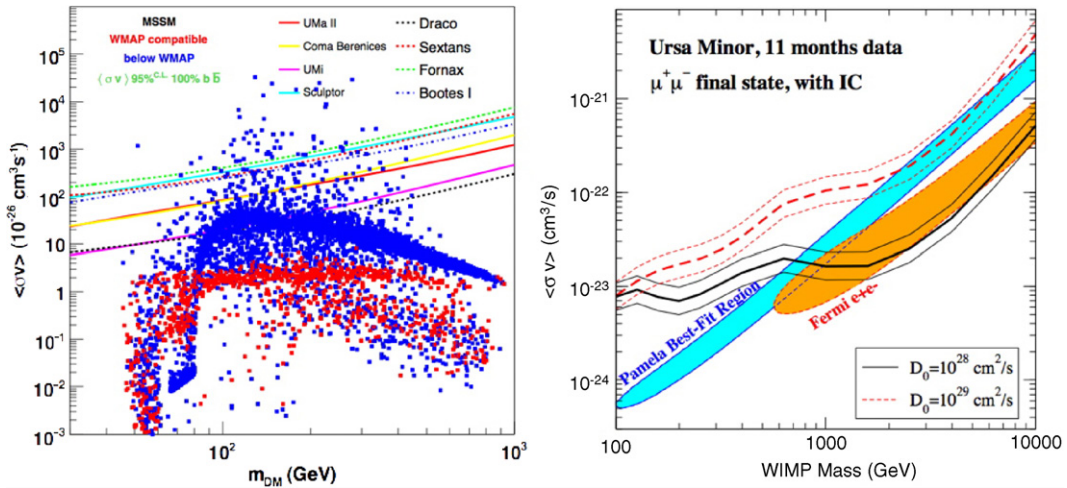


Fig. 9. (Left) MSSM models in the $(m_{wimp}, \langle\sigma v\rangle)$ plane consistent with all accelerator constraints. Red points have a neutralino thermal relic abundance corresponding to the inferred cosmological dark matter density (blue points have a lower thermal relic density, and we assume that neutralinos still comprise all of the dark matter in virtue of additional non-thermal production processes). The lines indicate the Fermi 95% upper limits obtained from likelihood analysis on the selected dwarfs. (Right) Constraints on the annihilation cross-section for a $\mu^+\mu^-$ final state based on the 95% confidence limits on the γ -ray flux compared to dark matter annihilation models which fit well either the PAMELA or Fermi $e^+ + e^-$ measurements. The constraints are for the Ursa Minor dwarf including both γ -ray emission from IC scattering and final state radiation. Here we consider two different diffusion coefficients and show the effect of the uncertainties in the Ursa Minor density profile.

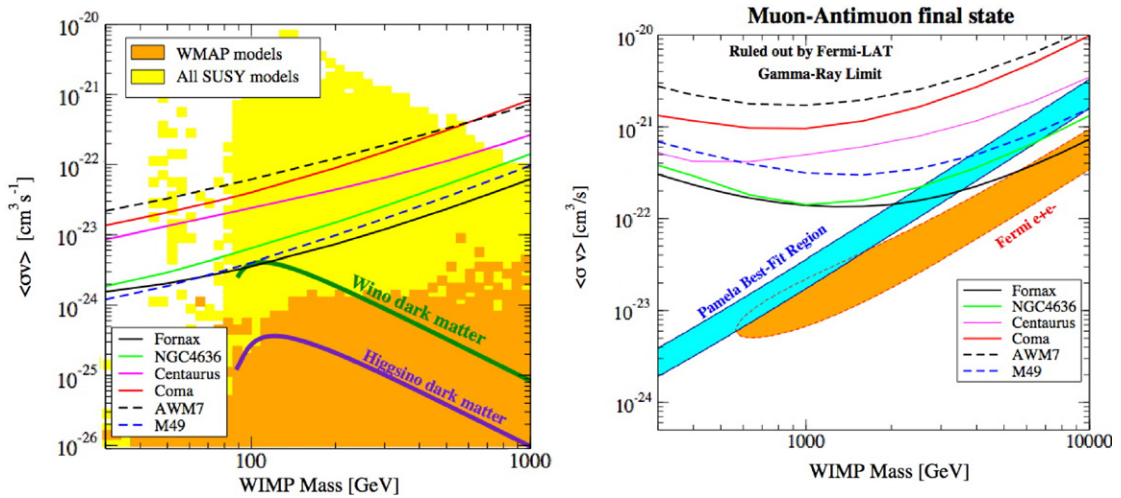


Fig. 10. Left: The expected gamma-ray spectrum from dark matter annihilation into a $\mu^+\mu^-$ final state including both FSR and emission from IC scattering of CMB photons for different assumed particle masses. The spectral normalization is arbitrary, but the same effective J is used in all cases. Right: Flux upper limits as a function of particle mass for an assumed $\mu^+\mu^-$ final state, including the contributions of both FSR and IC gamma-ray emission, for the clusters. The upper limits reflect the 95% confidence level limits on the photon flux in the 100 MeV–100 GeV energy range.

3. Dwarf spheroidal galaxies and clusters of galaxies

Local group dwarf spheroidal galaxies, the largest Galactic substructures predicted by the cold dark matter scenario, are attractive targets for dark matter indirect searches because they are nearby and among the most extreme dark matter dominated environments. With the data taken during the first 11 months no significant γ -ray emission was detected above 100 MeV from the candidate dwarf galaxies. So we can determine upper limits to the γ -ray flux assuming both power-law spectra and representative spectra from WIMP annihilation. The resulting integral flux above 100 MeV is constrained to be at a level below around 10^{-9} photons $\text{cm}^{-2} \text{ s}^{-1}$ [26]. Using recent stellar kinematic data, the γ -ray flux limits can be combined with improved determinations of the dark matter density profile in 8 of the 14 candidate dwarfs to place limits on the pair annihilation cross-section of WIMPs in several widely studied extensions of the standard model, including its supersymmetric extension and other models that received recent attention. With the present data we are able to rule out large parts of the parameter space where the thermal relic density is below the observed cosmological dark matter density and WIMPs (neutralinos here) are dominantly produced non-thermally, e.g. in models where supersymmetry

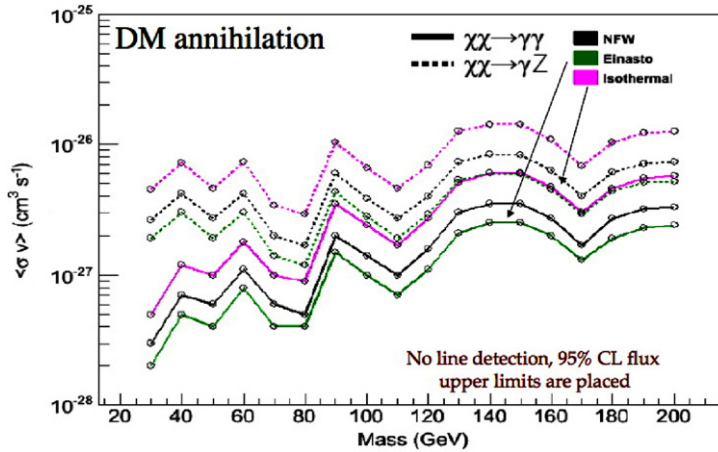


Fig. 11. Cross-section limits for various dark matter halo profiles for the annihilation in monochromatic gamma-rays.

breaking occurs via anomaly mediation. These γ -ray limits also constrain some WIMP models proposed to explain the *Fermi* and PAMELA e^+e^- data, including low-mass wino-like neutralinos and models with TeV masses pair-annihilating into muon-antimuon pairs (see Fig. 9).

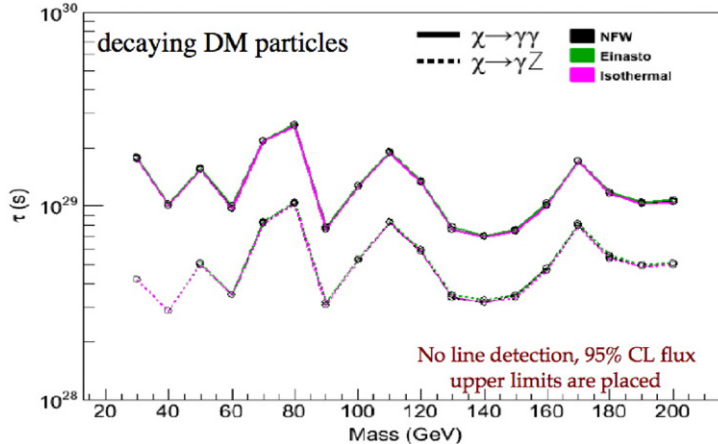


Fig. 12. Lifetime limits for various dark matter halo profiles for the decay in monochromatic gamma-rays channel.

The same kind of analysis can be done with the clusters of galaxies. Nearby clusters and groups of galaxies are potentially bright sources of high-energy gamma-ray emission resulting from the pair-annihilation of dark matter particles. However, no significant gamma-ray emission has been detected so far from clusters in the first 11 months of observations with the *Fermi* Large Area Telescope. We interpret this non-detection in terms of constraints on dark matter particle properties. In particular for leptonic annihilation final states and particle masses greater than ~ 200 GeV, gamma-ray emission from inverse Compton scattering of CMB photons is expected to dominate the dark matter annihilation signal from clusters, and our gamma-ray limits exclude large regions of the parameter space that would give a good fit to the recent anomalous *Pamela* and *Fermi-LAT* electron-positron measurements [27]. For an example see Fig. 10.

Finally a line at the WIMP mass, due to the 2γ production channel, could be observed as a feature in the astrophysical source spectrum [13]. Such an observation is a “smoking gun” for WIMP DM as it is difficult to explain by a process other than WIMP annihilation or decay and the presence of a feature due to annihilation into γZ in addition would be even more convincing.

Up to now however no lines were observed and we obtain γ -ray line flux upper limits in the range $0.6\text{--}4.5 \times 10^{-9} \text{ cm}^{-2} \text{ s}^{-1}$ [28] and corresponding DM annihilation cross-section and decay lifetime limits shown in Figs. 11 and 12.

4. Conclusion

Recent accurate measurements of cosmic-ray positrons and electrons by PAMELA, and *Fermi* have opened a new era in particle astrophysics. The CRE spectrum measured by *Fermi-LAT* is significantly harder than what was expected on the basis of previous data. Adopting the presence of an extra e^\pm primary component with ~ 2.4 spectral index and $E_{\text{cut}} \sim 1 \text{ TeV}$

allows one to consistently interpret Fermi-LAT CRE data, HESS and PAMELA. Such an extra-component can be originated by pulsars for a reasonable choice of relevant parameters or by annihilating dark matter for model with $M_{DM} \sim 1$ TeV. Improved analysis and complementary observations (CRE anisotropy, spectrum and angular distribution of diffuse γ , DM sources search in γ) are required to possibly discriminate the right scenario. Their exotic origin has to be confirmed by complimentary findings in γ -rays by Fermi and atmospheric Cherenkov telescopes, and by LHC in the debris of high-energy proton destructions. A positive answer will be a major breakthrough and will change our understanding of the universe forever. On the other hand, if it happens to be a conventional astrophysical source of cosmic rays, it will mean a direct detection of particles accelerated at an astronomical source, again a major breakthrough. In this case we will learn a whole lot about our local Galactic environment. However, independently on the origin of these excesses, exotic or conventional, we can expect very exciting several years ahead of us.

References

- [1] W.B. Atwood, et al., [Fermi Coll.], *Astrophys. J.* 697 (2) (2009) 1071–1102. [arXiv:0902.1089](#).
- [2] A.A. Abdo, et al., [Fermi Coll.], *Astropart. Phys.* 32 (2009) 193–219. [arXiv:0904.2226](#).
- [3] A.A. Abdo, et al., [Fermi Coll.], *Phys. Rev. Lett.* 102 (2009) 181101. [arXiv:0905.0025](#).
- [4] M. Ackermann, et al., [Fermi Coll.], *Phys. Rev. D* 82 (2010) 092004. [arXiv:1008.3999](#).
- [5] O. Adriani, et al., [PAMELA Coll.], *Nature* 458 (2009) 607. [arXiv:0810.4995](#).
- [6] A.W. Strong, I.V. Moskalenko, *Astrophys. J.* 509 (1998) 212; *Astrophys. J.* 493 (1998) 694.
- [7] A. Lionetto, A. Morselli, V. Zdravkovic, *J. Cosmol. Astropart. Phys.* 09 (2005) 010. [astro-ph/0502406](#); V.S. Ptuskin, et al., *Astrophys. J.* 642 (2006) 902.
- [8] A. Morselli, I. Moskalenko, *PoS(idm2008)025*. [arXiv:0811.3526](#).
- [9] A. Boulares, *Astrophys. J.* 342 (1989) 807–813.
- [10] F.A. Aharonian, A.M. Atoyan, H.J. Völk, *Astron. Astrophys.* 294 (1995) L41.
- [11] S. Coutu, et al., *Astropart. Phys.* 11 (1999) 429.
- [12] D. Grasso, et al., *Astropart. Phys.* 32 (2009) 140–151. [arXiv:0905.0636](#).
- [13] E. Baltz, et al., *JCAP07(2008)013*. [arXiv:0806.2911](#). 27.
- [14] M. Ackermann, et al., [Fermi Coll.], *Phys. Rev. D* 82 (2010) 092003.
- [15] A. Morselli, et al., *Nuclear Phys.* 113B (2002) 213.
- [16] A. Cesarini, F. Fucito, A. Lionetto, A. Morselli, P. Ullio, *Astropart. Phys.* 21 (2004) 267. [astro-ph/0305075](#).
- [17] <http://fermi.gsfc.nasa.gov/ssc/data/analysis/software/>.
- [18] A.A. Abdo, et al., [Fermi Coll.], *Astrophys. J. Suppl. Ser.* 188 (2010) 405. [arXiv:1002.2280](#).
- [19] A.S. trong, et al., *Astrophys. J.* 613 (2004) 962S.
- [20] A. Strong, et al., *Annu. Rev. Nucl. Part. Sci.* 57 (2007) 285.
- [21] V. Vitale, A. Morselli, for the Fermi/LAT Collaboration, 2009 Fermi Symposium. [arXiv:0912.3828](#).
- [22] A.A. Abdo, et al., [Fermi Coll.], *Astrophys. J.* 703 (2009) 1249–1256. [arXiv:0908.1171](#).
- [23] A.A. Abdo, et al., [Fermi Coll.], *Phys. Rev. Lett.* 104 (2010) 101101-1-7. [arXiv:1002.3603](#).
- [24] P. Sreekumar, et al., *Astrophys. J.* 494 (1998) 523.
- [25] A.W. Strong, I.V. Moskalenko, O. Reimer, *Astrophys. J.* 613 (2004) 956.
- [26] A.A. Abdo, et al., [Fermi Coll.], *Astrophys. J.* 712 (2010) 147–158. [arXiv:1001.4531](#).
- [27] M. Ackermann, et al., [Fermi Coll.], *JCAP, J. Cosmol. Astropart. Phys.* 05 (025) (2010) [arXiv:1002.2239](#).
- [28] A.A. Abdo, et al., [Fermi Coll.], *Phys. Rev. Lett.* 104 (2010) 091302-08. [arXiv:1001.4836](#).